

On the dependence of the dynamic crack tip temperature fields in metals upon crack tip velocity and material parameters¹

James J. Mason and Ares J. Rosakis

California Institute of Technology, 105-50, Pasadena, CA 91125, USA

Received 20 April 1992; revised version received 2 April 1993

Although various approximations have been used to analytically predict the temperature rise at a dynamic crack tip and its relation to the crack tip velocity or the material properties, few experimental investigations of these effects exist. Here, the method of using a high speed infrared detector array to measure the temperature distribution at the tip of a dynamically propagating crack tip is outlined, and the results from a number of experiments on different metal alloys are reviewed. First the effect of crack tip velocity in 4340 steel is investigated, and it is seen that the maximum temperature increases with increasing velocity, the maximum plastic work rate density increases with velocity and the active plastic zone size *decreases* with increasing velocity. Also, it is observed that a significant change in the geometry of the temperature distribution occurs at higher velocities in steel due to the opening of the crack faces behind the crack tip. Next, the effect of thermal properties is examined, and it is seen that, due to adiabatic conditions at the crack tip, changes in thermal conductivity do not significantly affect the temperature field. Changes in density and heat capacity (as well as material dynamic fracture toughness) are more likely to produce significant differences in temperature than changes in thermal conductivity. Finally, the effect of heat upon the crack tip deformation is reviewed, and it is seen that the generation of heat at the crack tip in steel leads to the localization of deformation in the shear lip. The shear lip is actually an adiabatic shear band formed at 45° to the surface of the specimen. In titanium, no conclusive evidence of shear localization in the shear lip is seen.

1. Introduction

It is known that in ductile metals plasticity ahead of a dynamically propagating or dynamically loaded crack can lead to the generation of heat resulting in a significant temperature rise at the crack tip. Such increases in thermal energy can lead to changes in fracture toughness, changes in fracture mode and instabilities in the resulting deformation. For example, it has been observed that heat generated in dynamic deformations can result in the decomposition of thermally unstable materials (Fox and Sonria-Ruiz, 1970) and local-

ized melting in titanium alloys (Bryant et al., 1986). If the conditions of the deformation are approximated by neglecting heat conduction (by assuming that adiabatic heating conditions prevail) and by neglecting the thermo-elastic effect, the temperature rise due to dynamic plasticity is given quite simply by

$$\Delta T(t) = \frac{1}{\rho c_p} \int_{-\infty}^t \beta \sigma_{ij}(\tau) \dot{\epsilon}_{ij}^p(\tau) d\tau, \quad (1)$$

where $\Delta T(t)$ is the temperature rise, β is the fraction of work converted to heat – roughly 0.85–1.00 (Taylor and Quinney, 1934; Bever et al., 1973) – ρ is the density (assumed independent of temperature), c_p is the specific heat (also assumed independent of temperature), and σ_{ij} and $\dot{\epsilon}_{ij}^p$ are the cartesian stress and plastic strain-rate tensor components. The temperature field in

Correspondence to: Dr. A.J. Rosakis, Graduate Aeronautical Laboratories, California Institute of Technology, Pasadena, CA 91125, USA.

¹ Research performed with support from the Office of Naval Research under Grant N00014-90-J-1340.

this case corresponds exactly with the plastic deformation field; when the plastic work density is higher the temperature is higher, and there is no temperature rise at a point if no plasticity occurs there. While the assumption of adiabatic heating may significantly simplify the problem of calculating the temperature rise in dynamic deformation experiments, the conduction of heat is not completely absent in any realistic situation. If the effects of heat conduction are included in the analysis, the standard heat (or diffusion) equation is invariably invoked,

$$\alpha \nabla^2 T - \frac{\partial T}{\partial t} = - \frac{\dot{W}^p}{\rho c_p}, \quad (2a)$$

where $\alpha = k/\rho c_p$, k is the thermal conductivity, and

$$\dot{W}^p = \beta \sigma_{ij} \dot{\epsilon}_{ij}^p. \quad (2b)$$

On the right-hand side of this equation is the term characterizing a source of heat in plastic deformation (Taylor and Quinney, 1934; Bever et al., 1973). The solution of this coupled heat equation is greatly dependent upon the geometry of the problem at hand. For a crack of length a , propagating at a constant velocity, \dot{a} , it is beneficial to use a coordinate system that is translating with the crack tip. This results in a reformulation of Eq. (2a):

$$\alpha \nabla^2 T + \dot{a} \frac{\partial T}{\partial x_1} = - \frac{\dot{W}^p}{\rho c_p}, \quad (3)$$

x_1 is the coordinate parallel to the crack faces and x_2 is perpendicular to the crack faces with the origin at the crack tip. The solution of Eq. (3) for a point source of heat in two dimensions is given by Carslaw and Jaeger (1959) as

$$T_p(x_1, x_2) = \frac{\dot{Q}}{2\pi k} \exp\left(-\frac{\dot{a}x_1}{2\alpha}\right) K_0\left(\frac{\dot{a}r}{2\alpha}\right), \quad (4)$$

where $r = \sqrt{x_1^2 + x_2^2}$ and K_0 is the modified Bessel's function of the zeroth order. To predict

the temperature field around a propagating crack tip the point source solution is used as a Green's function to be integrated over the area of the plastic work zone, A_p . Assuming the plastic work zone is self-similar throughout the thickness of the specimen and letting $\dot{Q} = \dot{W}^p d\xi_1 d\xi_2$, the temperature field due to a experimental plastic zone is given by

$$T(x_1, x_2) = \int_{A_p} T_p(x_1 - \xi_1, x_2 - \xi_2) \times \dot{W}^p(\xi_1, \xi_2) d\xi_1 d\xi_2. \quad (5)$$

Because of the logarithmic singularity of the modified Bessel's function at $r = 0$, the solution given by Eq. (5) is finite and well behaved. Note that the assumption of a through-thickness, self-similar plastic work zone is rarely true where experimental temperature measurements are made – at the surface – due to the stress free surface boundary condition. Also note that knowledge of the active plastic zone size and shape, $\dot{W}^p(x_1, x_2)$ is required in Eq. (5). Exactly determining this function in closed form for most real materials is virtually impossible. Approximations are used, or numerical calculations are substituted. A summary of some of the theoretically predicted temperature rises reported in the literature can be

Table 1

Some predictions of the temperature rise at the tip of a dynamically propagating crack

References	Material	Crack speed (m/s)	Maximum temperature (°C)
Rice and Levy, 1969	steel	900	1400
	titanium	900	> 10000
Kuang and Atluri, 1985	steel	762	700
Sung and Achenbach, 1987	steel	300	700
Douglas and Mair, 1987	steel	1500	1
	titanium	1500	50
Malali, 1988	steel	1500	528
	titanium	1500	11500
Krishna Kumar et al., 1991	steel	320–1600	150–400

found in Table 1. Notice that for titanium the predicted temperature rise is typically very large. It has been suggested that this effect is due to the low thermal conductivity of titanium when compared to steel. Also notice that there is a large variation in the predicted temperature and the predicted dependence of the temperature rise upon crack speed. It is clear that experimental measurement of the maximum temperature rise at a dynamically propagating crack tip is necessary to help clarify the present understanding of this phenomenon. For the case of a crack propagating in steel, the theoretical temperature field may be calculated using an experimental approximation of the plastic work zone (Mason and Rosakis, 1992) as shown in Fig. 1. Notice that the contours of constant temperature extend straight back from the theoretical plastic zone curving toward the negative x_1 axis some distance behind the crack tip. This solution differs from the adiabatic solution only in that the temperature is forced to zero at $r = \infty$ due to the boundary conditions of the point source solution in Eq. (4).

2. Experimental methods

The measurement of the temperature field at a dynamic crack tip (a crack tip that is either propagating or dynamically loaded) requires some specific properties from the measurement apparatus. First, it is necessary that the measurement technique does not significantly alter the deformation field or the temperature field. Thus, it must be a non-destructive technique; drilling a hole for a thermocouple, for example, is not feasible. Second, it is necessary that the system be capable of fast response times. For a crack propagating at 900 m/s the temperature could rise from zero to its maximum in 2 μ s. A rise time of at least 1 μ s in the measuring system is required. Candidate methods include; thermocouples on the surface, thermally sensitive films and infrared detector. For a complete discussion of these techniques see Mason (1993), the results reported here use the infrared detector array system employed by Zehnder and Rosakis (1991, 1992) and Zehnder and Kallivayalil (1991). This

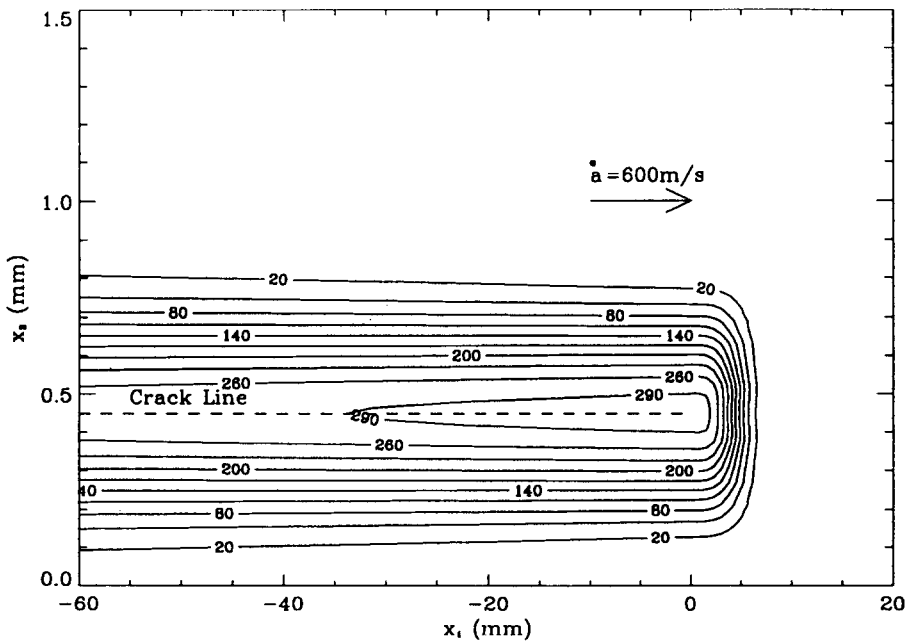


Fig. 1. Theoretical calculation of the temperature field around a propagating crack tip in steel (Mason and Rosakis, 1992). A convolution of the the form in Eq. (5) is used in conjunction with an approximation to the experimentally measured plastic work zone shown in Figs. 6 and 7.

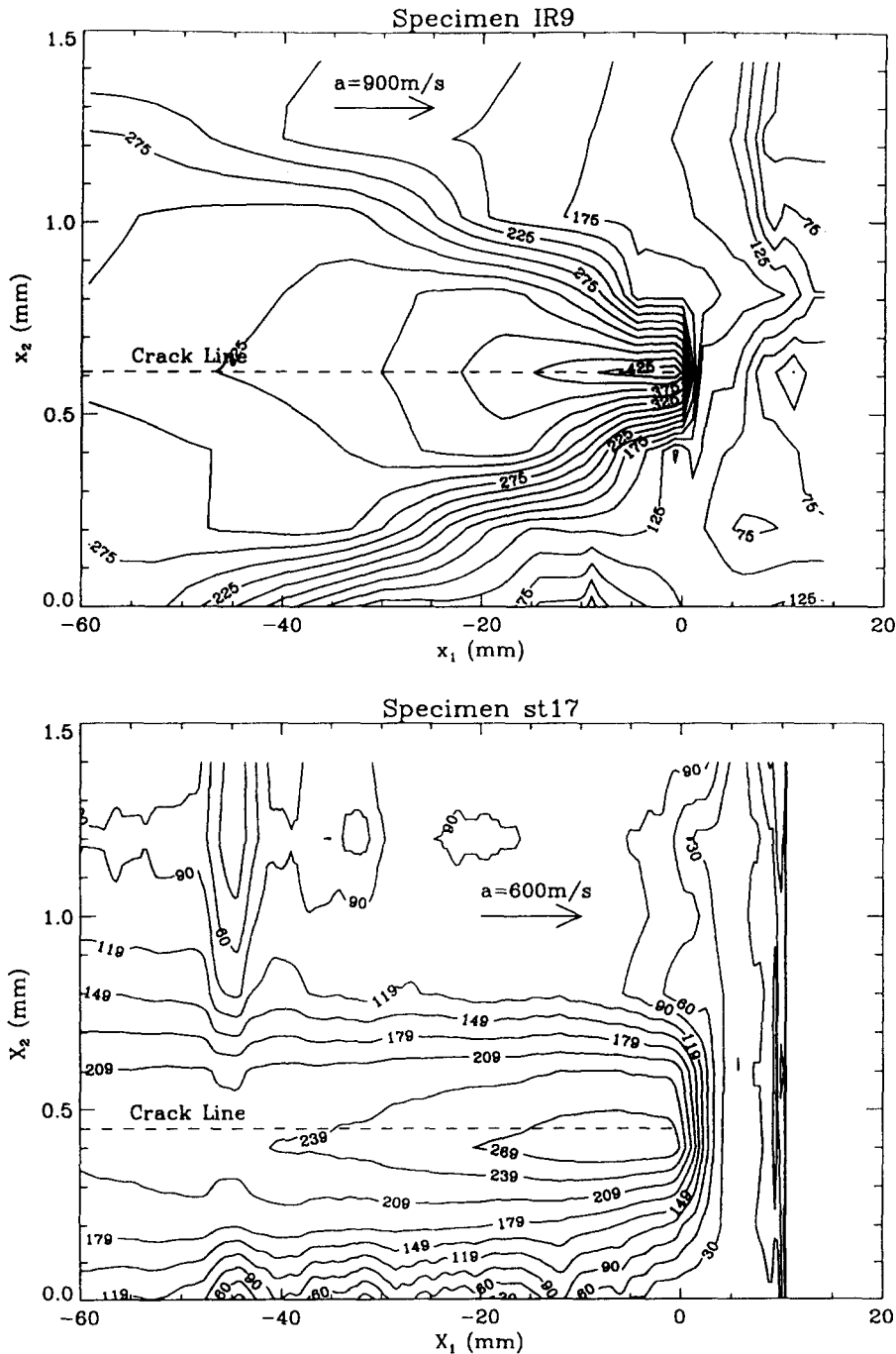


Fig. 2. Temperature distribution measured experimentally using infrared detectors around a crack tip propagating in 4340 oil-quenched steel at a velocity of 900 m/s (Zehnder and Rosakis, 1991) and 600 m/s. Maximum temperatures of approximately 450°C at 900 m/s and 300°C at 600 m/s are observed. The crack line location in the vertical direction is estimated from the symmetry of the results. The temperature rise at $x_2 \approx 1.2$ mm in the slower velocity experiment is due to the formation of another shear lip. Note that this formation occurs behind the crack tip at distances at least as large as 20 mm.

systems is based on the system used by Duffy and coworkers (Duffy, 1984; Hartley et al., 1987; and Marchand and Duffy, 1988) to measure the temperature rise in dynamically shearing cylinders loaded in torsion. An Offner (Offner, 1975) imaging system is used in conjunction with a linear array of InSb detectors. The detectors integrate over a range of wavelengths; for InSb that range is 1 μm to 5.5 μm . The voltage produced by the detectors is related to the energy emitted by the specimen through an integral depending upon the emissivity of the material, $\epsilon(\lambda, T)$, the spectral response of the InSb detector, $R(\lambda)$, and the black body radiation function, $P(\lambda)$, where λ is the wavelength of the radiation:

$$v(T, T_0) = AA_D \beta \int_{1 \mu\text{m}}^{5.5 \mu\text{m}} R(\lambda) [P(\lambda, T) \epsilon(\lambda, T) - P(\lambda, T_0) \epsilon(\lambda, T_0)] d\lambda, \quad (6)$$

where A is the amplification, A_D is the detector area and β is the fraction of energy transmitted to the detectors by the optical system (related to the aperture). This relation when evaluated for InSb detectors produces a nearly linear relation on a log-log plot (Zehnder and Rosakis, 1991, 1992). By simply heating a specimen, measuring its surface temperature with a thermocouple, and plotting the results on a log-log plot, one may establish a calibration curve for the detectors that eliminates the need to evaluate the emissivity of the sample, the spectral response of the detector and the black body radiation function. Using this calibration, the voltage record of a detector during a test may be trivially converted into a temperature measurement.

In order to protect the infrared detector imaging system from the dangers of impact loading, dynamic cracks are produced by statically wedge loading a compact tension specimen with a blunt notch. The speed of the crack can be roughly controlled by changing the radius at the notch tip; a blunt notch produces a faster crack than a sharp notch. Dynamic cracks are produced by the storage of elastic energy at the notch tip prior to failure; as the load is increased more elastic energy is stored in the specimen. When a small crack initiates at the notch tip, the excess elastic

Table 2
Tensile properties

Material and condition	σ_y (MPa)	σ_u (MPa)	ϵ_u (%)	K_{Ic} (MPa \sqrt{m})
4340, quenched ^a		1700		44
Ti, 0% α_p ^b	1370	1390	0.35	56

^a Zehnder and Rosakis (1991).

^b Giovanola et al. (1989).

energy drives the crack dynamically through the specimen. The notch radius is machined by conventional EDM techniques giving a reproducible notch root radius. A minimum radius of 0.25 mm is attainable resulting in a minimum crack speed of 600 m/s in the 4340 steel studied here. Crack speed is measured by a series of conducting break-lines on the back surface of the sample (see Zehnder and Rosakis, 1991, 1992, and Zehnder and Kallivayalil, 1991).

3. Results and discussion

The results of four testing conditions are reviewed here. In Fig. 2a the results of Zehnder and Rosakis (1991) are recalled, and in Fig. 2b the results of a recent investigation by the authors are shown. The material in both experiments is the same, oil-quenched 4340 steel with hardness $R_c = 44$ (see Tables 2–4), but the crack speed is 900 m/s in the Zehnder and Rosakis (1991) experiment while the crack speed is 600 m/s here. These results are representative of a number of experiments. In the latter case four separate experiments were performed, some with different apertures, to show the repeatability of the results. (Temperature rises below 50°C fall

Table 3
Elastic properties

Material and condition	E (GPa)	ν	ρ (kg/m ³)
4340, quenched ^a	210	0.30	7830
Ti, 0% α_p ^{b,c}	110	0.32	4650

^a Battelle Columbus Laboratories (1989), *Aerospace Structural Metals Handbook*.

^b Bryant et al. (1986).

^c American Society for Metals (1980), *Metals Handbook*.

below the noise level of the system.) It can be seen that the two fields are significantly different. Most noticeable is the triangular arrangement of

the temperature contours behind the crack when $\dot{a} = 900$ m/s. Contours emanating from the crack tip expand outward initially before curving back

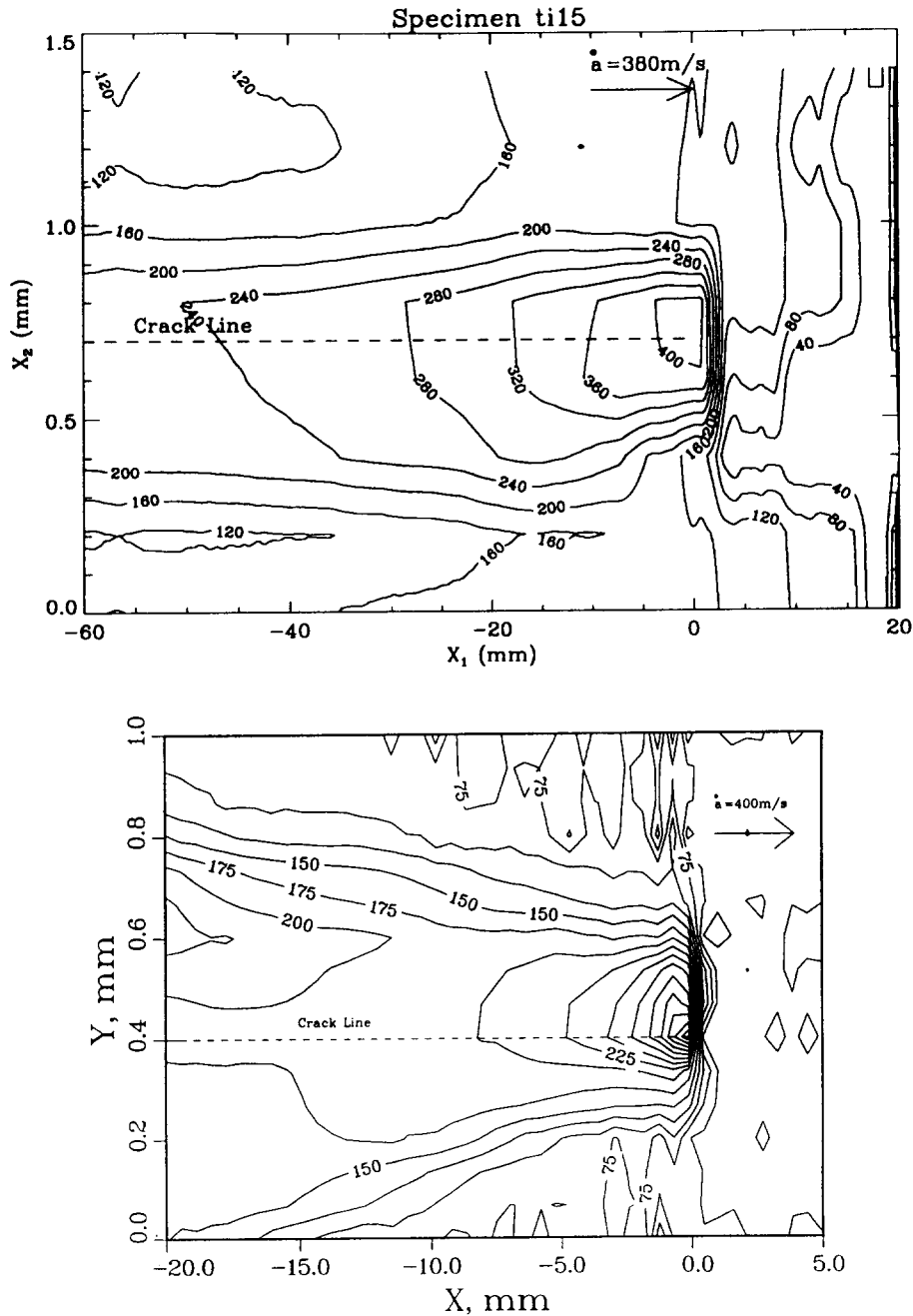


Fig. 3. The temperature field around a crack tip propagating at 380 m/s in Ti-10V-2Fe-3Al alloy and 400 m/s in beta-C Ti (Zehnder and Kallivayalil, 1991). Some of the detectors were saturated in the Ti 10V-2Fe-3Al test, but a maximum temperature of approximately 500°C may be extrapolated from the results. In the beta-C Ti material a maximum temperature of 260°C is reported.

Table 4
Thermal properties

Material and condition	c_p (J/kg °C)	k (W/m °C)	α ($\mu\text{m}^2/\text{s}$)	κ ($\mu\text{m}/\text{m}^\circ\text{C}$)
4340, quenched ^a	448	34.6	9.86	11.2
Ti, 0% α_p ^{b,c}	490	10.9	4.78	9.7

^a Battelle Columbus Laboratories (1989), *Aerospace Structural Metals Handbook*.

^b Bryant et al. (1986).

^c American Society for Metals (1980), *Metals Handbook*.

to meet the negative x_1 axis. Similar contours are not seen for a $\dot{a} = 600$ m/s or in Fig. 1. At 600 m/s an interesting feature of the temperature field is seen along the horizontal line, $x_2 = 1.2$. Here the temperature rise due to the formation of another “shear lip” is observed. This formation occurs behind the crack tip and is much less intense in terms of plastic work rate density. Examination of the specimen after failure reveals that the “other shear lip” follows a path parallel

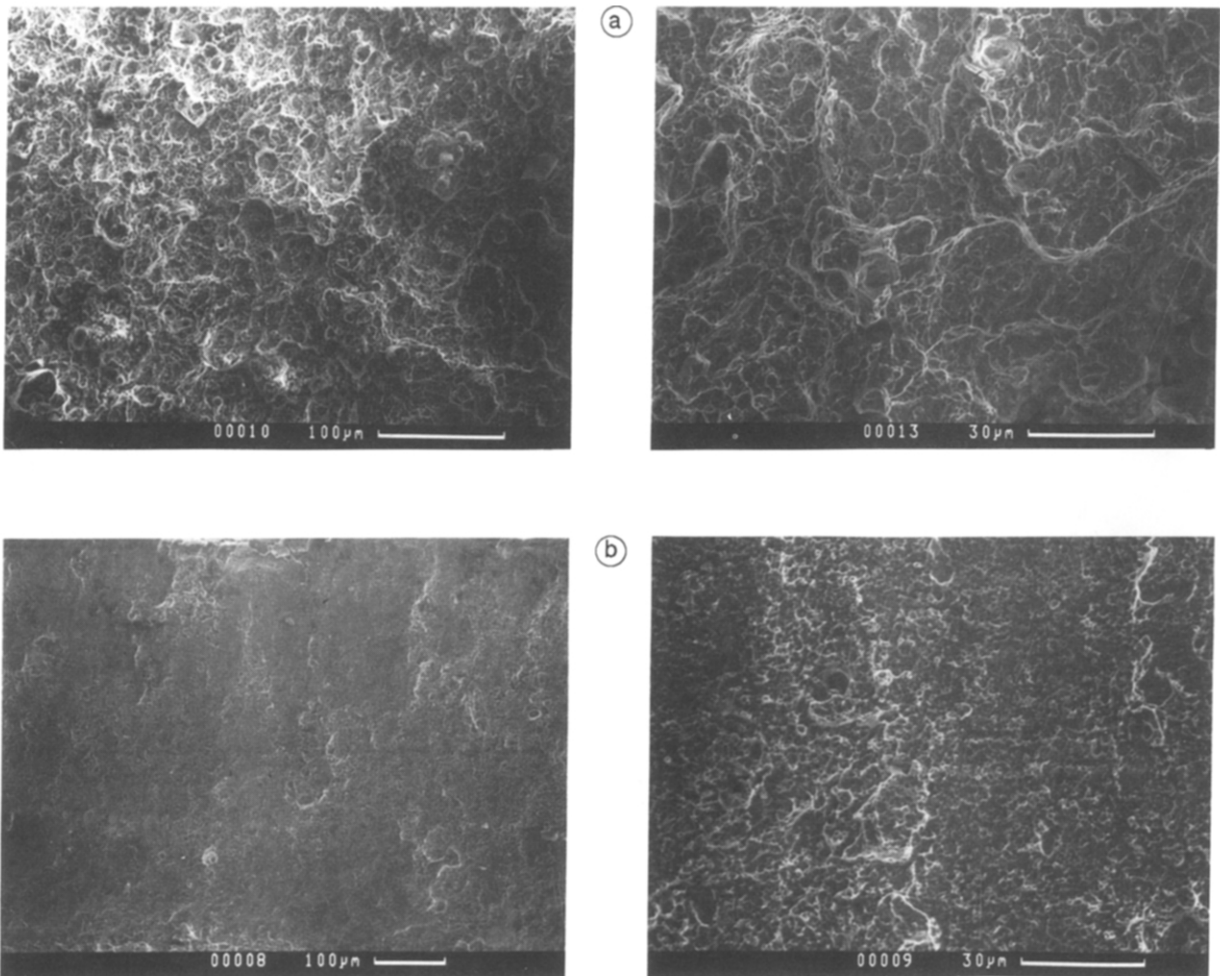


Fig. 4. Examination of the fracture surfaces in steel reveals different fracture morphology (a) in the flat fracture region than (b) on the shear lips. The smoother fracture surface in the shear lips indicates the formation of a shear band as seen in Giovanola (1988, 1988b).

to the crack path, and the separation between shear lips is approximately 0.75 mm for cracks propagating at 600 m/s while for crack propagating at 900 m/s the separation is closer to 1.2 mm. The maximum temperature for 900 m/s is 450°C while the maximum temperature for 600 m/s is 300°C. The crack tip positions are estimated from the crack tip displacement record. This method is not very accurate and the crack tip location uncertainty may be as much as 0.5 mm.

In Fig. 3 the results of some experiments on two separate titanium alloys are shown. In the first case a Ti-10V-2Fe-3Al alloy was tested in

the 0%- α_p state (Giovanola et al., 1989) (see Tables 2-4.) The crack speed is 380 m/s and the maximum temperature is greater than 400°C (the detectors saturated). In the second case the results of Zehnder and Kallivayalil (1991) for beta-C titanium are shown. The crack speed is 400 m/s, and the maximum temperature is 260°C. The results for Ti-10V-2Fe-3Al bear resemblance to the results for 4340 at 600 m/s as well as the theoretical result shown in Fig. 1. Contours extend directly back from the plastic zone roughly parallel to the crack faces eventually curving in to meet at the negative x_1 axis. In contrast, the

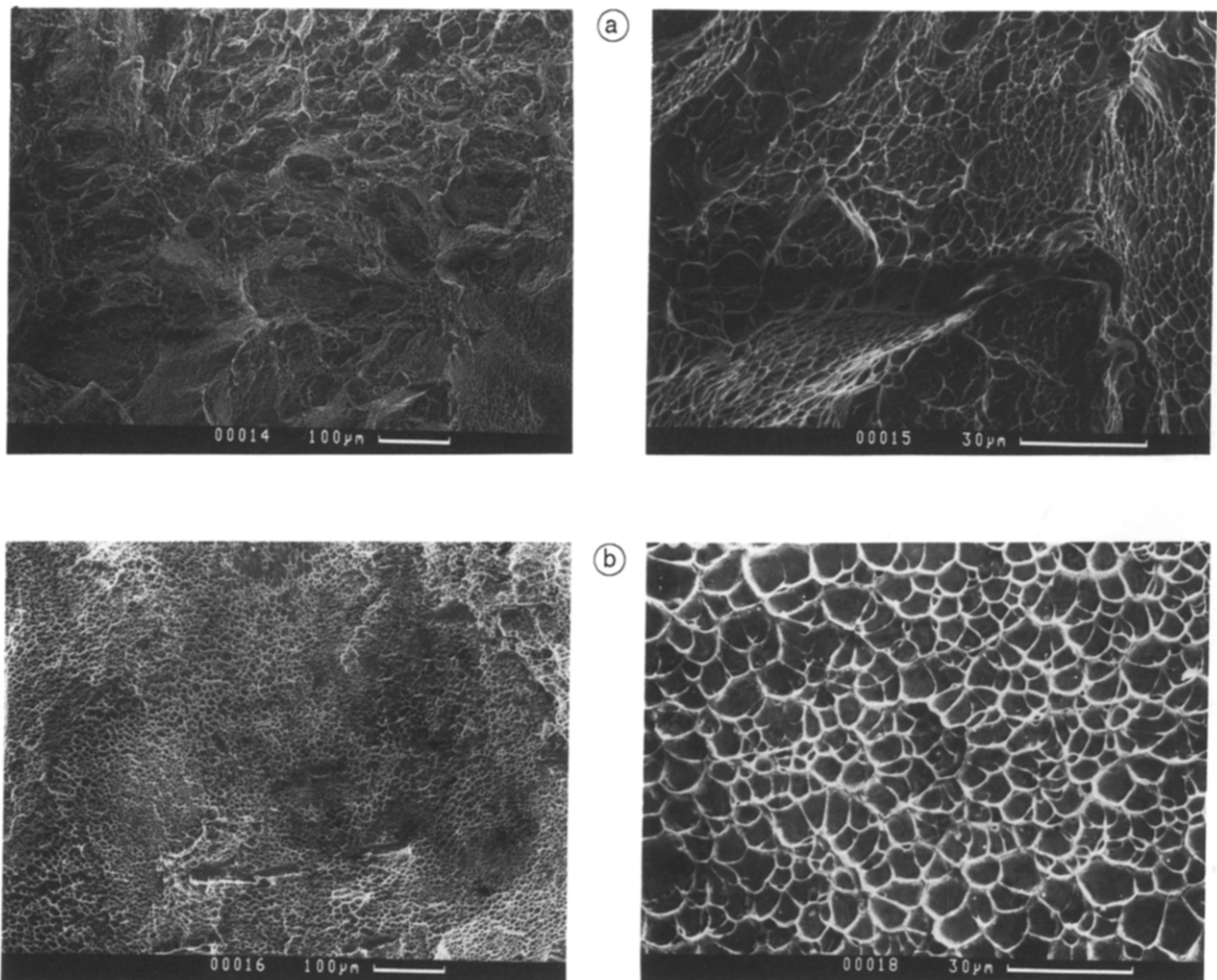


Fig. 5. The fracture surfaces in Ti-10V-2Fe-3Al reveal very similar fracture in: (a) the flat fracture region; and (b) the shear lip. However, more evidence of ductile void growth is evident in the shear lip and a more tortuous path is seen in the flat fracture regime.

contours in the experiment on beta-C titanium emanate outwardly as for 4340 steel at 900 m/s. Further, the existence of a shear localization above the crack tip due to the stress state at the surface of the specimen (Zehnder and Rosakis, 1991) is seen. This "other shear lip" is seen to curve out of the field of view behind the crack tip unlike the "other shear lip" observed in the experiments on 4340 steel at 600 m/s. The shear lips formed in the testing of beta-C titanium are much smaller than those formed in the testing of Ti-10V-2Fe-3Al. In the beta-C it can be seen in the figure that the shear lips are approximately 0.5 mm wide while in Ti-10V-2Fe-3Al examination after testing reveals that the shear lips can be as much as 4 mm wide. (That is, the shear lip height was less than 2 mm.)

Fractographic analysis of the shear lips offers some interesting comparisons. In Fig. 4 the fracture surface of the steel specimen at $\dot{a} = 600$ m/s may be seen both in the flat fracture regime and in the shear lip. It can be seen that there is a drastic difference in the two surfaces. In the flat fracture regime, the surface is rough and the crack path is tortuous. Regions of microvoid coalescence may be observed. On the shear lip, smooth surfaces dominate. (It is interesting to note that the two faces of the shear lip probably do not smear each other after failure has occurred since the crack is loaded in the mode I or "opening mode." The crack faces immediately separate upon failure.) This fracture is similar to the fracture surface reported by Giovanola (1988, 1988b) for a shear band in the same material with a different heat treatment. Giovanola reports the existence of "cobble regions" as well as microvoid coalescence regions that are not seen here, but it is clear that the two fracture modes are the same. In the titanium, Fig. 5, the flat fracture regime exhibits a tortuous crack path with regions of microvoid coalescence visible along the walls of the peaks and valleys, but in the shear lip fracture is dominated by microvoid coalescence. The voids on the shear lip are much larger than those in the bulk fracture region. None-the-less, it is clear that microvoid coalescence in shear is important in both regions. Thus, the two regions are similar.

3.1. Temperature fields in steel

The most striking difference between Figs. 2a and 2b is the existence of triangular contours emanating from the crack tip in the temperature field at the higher velocity. Because the velocity of the crack is extremely high when compared to the material properties ($\dot{a}\delta\rho c_p/2k \gg 1$, see Mason and Rosakis, 1992) in both figures it is expected that *both* fields should reflect the qualitative behavior exhibited in Fig. 1 (Mason and Rosakis, 1992). The contour lines should extend directly back from the plastic zone parallel to the crack faces until they eventually curve toward the negative x_1 axis some distance behind the crack tip. This behavior is seen in Fig. 2b, but it is *not* seen in Fig. 2a.

Owing to the heavy dependence of theoretical maximum temperatures upon the assumptions about the plastic zone, it was initially thought that the difference in contours between Figs. 2a and 2b might be due to a difference in plastic zone. Unfortunately, estimates of the plastic zone show no difference between the plastic deformation at high and low velocities that could explain the change in the contours. Further, attempts to explain the difference in temperature field at high and low velocities using hyperbolic heat conduction have shown that this theory is not effective in modelling the observed behavior (Mason and Rosakis, 1992). It seems that the change in temperature field at the higher velocities is due to movement of the crack faces. It has been shown by Freund (1977) that, qualitatively, the crack opening velocity should be proportional to the crack velocity and the initial crack tip stress intensity factor. Clearly the crack tip velocity is higher in one case, but, also, the initial stress intensity factor may be as much as three times higher when $\dot{a} = 900$ m/s than when $\dot{a} = 600$ m/s (Rosakis and Zehnder, 1985). Combined, these two effects predict that the crack opening velocity in the 900 m/s test may be 5 times higher than that in the 600 m/s test. From the angle of the contours it is estimated that the average velocity of the crack faces in the x_2 direction is 7.5 m/s when the crack tip velocity is 900 m/s and less than 2 m/s when the crack tip velocity is

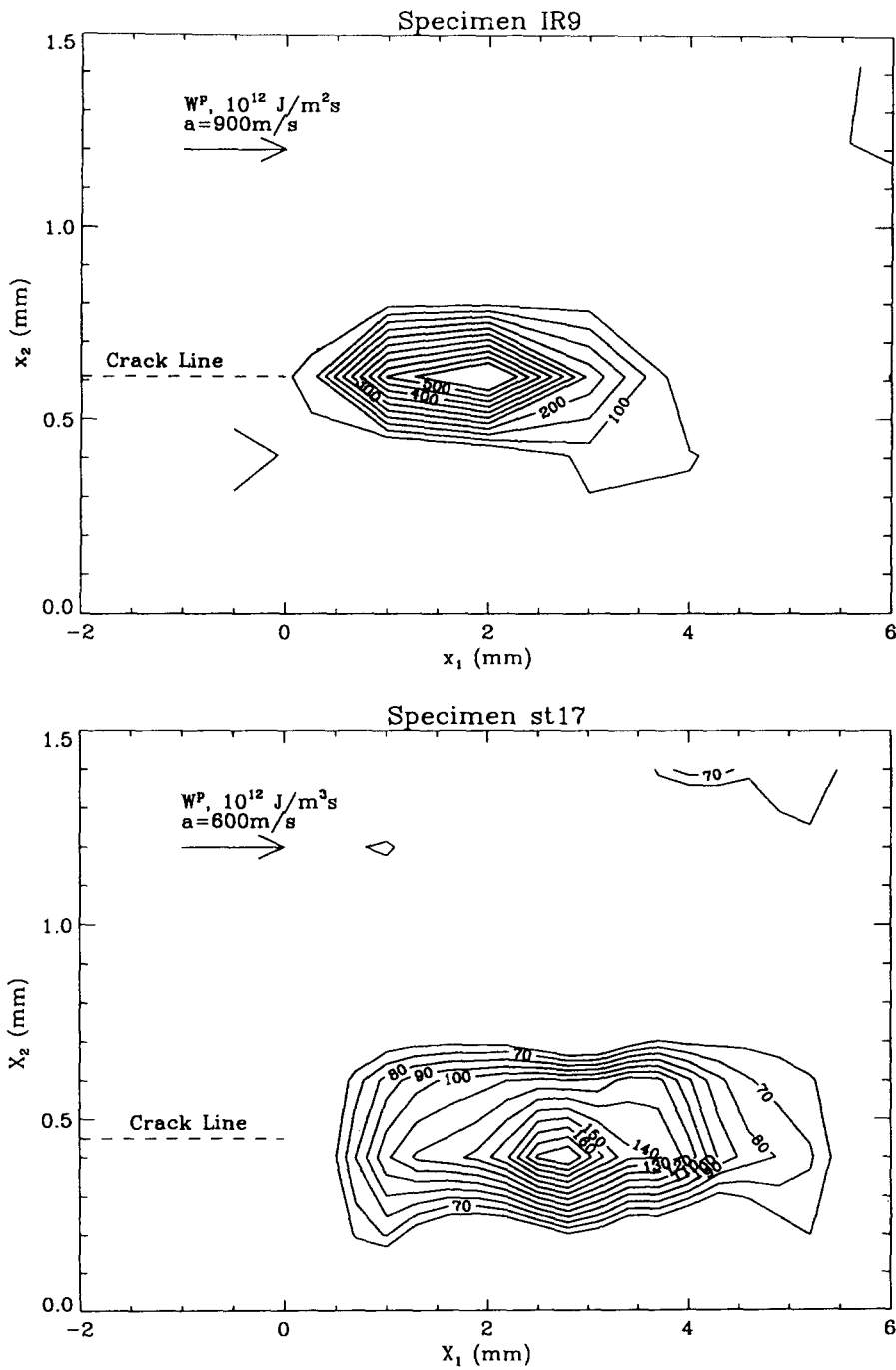


Fig. 6. The plastic work zone as estimated from Eq. (7) is shown for a crack propagating in oil-quenched 4340 steel at two velocities; 900 m/s and 600 m/s. It is seen that the plastic zone is elongated in the x_1 direction and that although the shape is the same at both velocities the zone at higher velocities is smaller reflecting a localization of plastic deformation as velocity increases.

600 m/s resulting in a ratio of crack face velocities greater than 4. Inaccuracies are expected when comparing this simple theory with the experimental results. The specimen is much more complex in the experiment than in the theory and measurements of the initiation stress intensity factor were not made. Consequently, it is concluded here that crack opening is responsible for the change in temperature field at the higher velocity, however, no quantitative analysis of this effect is implied.

The plastic work rate ahead of the crack tip may be estimated by using Eq. (3) and neglecting conduction (Zehnder and Rosakis, 1991, 1992; and Zehnder and Kallivayalil, 1991). Letting $\alpha = 0$ in this equation yields

$$-\rho c_p \dot{a} \frac{\partial T}{\partial x_1} = \beta \sigma_{ij} \dot{\epsilon}_{ij}^p. \quad (7)$$

Solving this relation for the experimental results in Fig. 2 gives the results shown in Fig. 6. For steel β is taken to be 0.9; this choice is justified

by some preliminary results of a split-hopkinson pressure bar investigation of this material parameter (Mason et al., 1992). It is seen that the plastic zone is approximately twice as large in the lower velocity experiment as it is in the higher velocity experiment. The fact that they are almost exactly twice as large in the x_2 direction is due to discretization of the temperature field by the finite detectors. It can only be said that at the lower velocity there is a larger plastic zone than at the higher velocity. The maximum plastic work density rate in the high speed test is 600×10^{12} J/m³ s while in the low speed test the maximum is 200×10^{12} J/m³ s, a third as much. The change in maximum plastic work rate density and the change in the x_2 dimension of the plastic work zone in conjunction with the fractography seen in Fig. 4 indicate that the shear lip is actually a shear band. A localization of the deformation is observed as crack velocity increases indicating the formation of an adiabatic shear band.

Estimation of the energy fraction consumed by the formation of the shear lips (Zehnder and

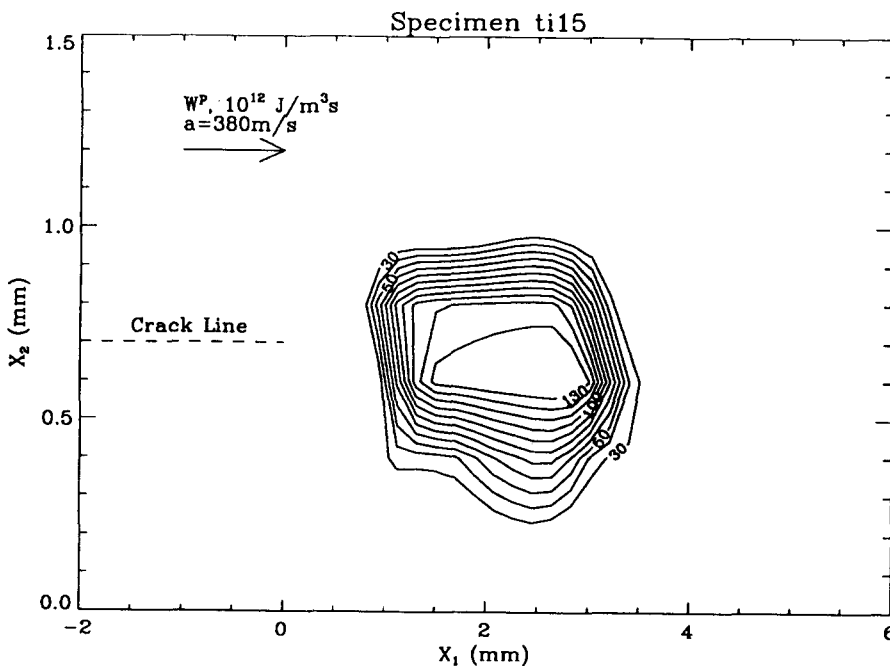


Fig. 7. The plastic zone for Ti-10V-2Fe-3Al is estimated as in Eq. (7). The zone shows similarity in shape to the results for 4340 steel in Fig. 6. The magnitude of the plastic work is the same as for oil-quenched 4340 steel with a crack propagating at 600 m/s, but the temperature is higher because the factor $\rho c_p \dot{a}$ is smaller in the Ti-10V-2Fe-3Al.

Rosakis, 1991) shows that roughly the same fraction of energy is expended in the shear lips in both the high and low speed experiments. Values for the energy expended in the lips during low speed fracture were, in general, slightly higher than the high speed experimental results, but, within the large uncertainty of the calculation, the two are equal. Regardless, a surprisingly large percentage, 50%, of the energy of dynamic fracture is expended in the shear lips during fast fracture. This is surprising because the area of the shear lips accounts for only about 10% of the fracture surface area in both experiments.

3.2. Temperature fields in titanium

In titanium the plastic zone is quite similar in size and shape to the plastic zones in steel; see Fig. 7. The maximum plastic work rate density for a crack propagating at 380 m/s in the tough titanium alloy is estimated – since the detectors saturated – to be approximately equal to the maximum plastic work rate density in 4340 steel at 600 m/s while the maximum temperature is greater than 400°C in Ti compared to 300°C in steel. Since adiabatic conditions apply at the crack tip (this is readily shown by comparing the magnitude of two terms on the left-hand side of Eq. (3)), it is expected that Eq. (7), which has no dependence upon thermal conductivity, k , should apply. Thus, the temperatures are *higher* in Ti than in steel when plastic work rates are roughly equal, however they are not higher because of the lower thermal conductivity. The temperature is actually higher because the factor $\rho c_p \dot{a}$ is smaller in the titanium; in titanium $\rho c_p \dot{a} = 8.7 \times 10^8$ J/m² s °C while in steel $\rho c_p \dot{a} = 21.0 \times 10^8$ J/m² s °C, roughly twice that in titanium.

Bryant et al. (1986) indicate evidence of localized melting in the Ti–10V–2Fe–3Al alloy used here, but fractographic examination in Fig. 5 gives no indication of melting in the shear lips or the flat fracture region. This may be due to differences in heat treatment.

In the experiments by Zehnder and Kallivayalil (1991) on beta-C titanium the existence of a shear lip above the actual crack demonstrates

that crack face opening has an effect on the measurement of temperature field. The shear lip is seen to curve out of the field of view. Since it is certain that near adiabatic conditions apply and that shear lip formation occurs parallel to the crack path, it is concluded that this movement is due to a translation of the crack faces rather than a change in the deformation. Thus, crack face opening effects are seen in beta-C titanium at 400 m/s supporting the conclusion that crack face opening is seen in the steel tests at 900 m/s.

4. Conclusions

(1) The maximum plastic work rate density increases with crack velocity for tests performed on a crack propagating at 600 m/s and 900 m/s in 4340 steel.

(2) The plastic zone size, however, decreases with increasing crack tip velocity for the same experiments.

(3) It is observed that the temperature field around a dynamically propagating crack tip in oil-quenched 4340 steel changes significantly when the crack velocity is increased from 600 m/s to 900 m/s. This effect is attributed to the faster crack opening rate at higher velocities. Conclusive evidence of crack face opening is seen in the temperature fields of Zehnder and Kallivayalil for beta-C titanium (Zehnder and Kallivayalil, 1991), and, furthermore, it is predicted by a simple theory that crack face opening will be much more significant at 900 m/s than at 600 m/s in 4340 steel. The effects of crack face opening have been ignored in experimental investigations of this kind up to now, and this conclusion demonstrates that such effects cannot always be neglected.

(4) In titanium the generation of heat at the tip of a dynamically propagating crack has been investigated. The maximum temperature in Ti–10V–2Fe–3Al for equivalent maximum plastic work rate densities is higher than in 4340 steel. Because of the adiabatic conditions at the crack tip this effect is not attributed to the lower thermal conductivity, rather it is attributed to the lower crack speed, the lower density and the

lower heat capacity of titanium though the factor $\rho c_p \dot{a}$. (See Eq. (7)).

(5) It is clear that the shear lip formed in oil-quenched 4340 steel is actually a shear band, a localization of the shear deformation to a narrow plane as a result of thermal softening in the material. At lower velocities the localization is less pronounced and the maximum temperature measured is lower. Fractography indicates a shear band fracture mode in the shear lip but not in the flat fracture regime.

(6) In Ti-10V-2Fe-3Al in the shear lips, failure is dominated by nucleation and growth of large micro-voids while in the bulk, flat-fracture region, failure occurs by the nucleation and growth of smaller micro-voids and a more tortuous crack path. Large micro-voids generate more plasticity than small voids, so it is expected that temperatures will be higher when microvoid growth is more extensive, in the shear lip. The shear lip in this case may or may not be formed as the result of shear localization. The evidence is, thus far, inconclusive.

Acknowledgements

We are grateful to A.T. Zehnder for sharing the raw data from his investigation and to J. Kallivayalil and A.T. Zehnder for sharing figures from their work together. The computations described here were carried out on a Cray Y-MP at the San Diego Supercomputing Center (SDSC).

References

- Battelle Columbus Laboratories, (1989), *Aerospace Structural Metals Handbook*, Metals and Ceramics Information Center, Columbus, OH, Vol. 1, Code 1206.
- Bever, M.B., D.L. Holt and A.L. Titchener (1973), The stored energy of cold work. *Prog. Mater. Sci.*, 17, 1.
- Bryant, J.D., D.D. Makel and H.G.F. Wilsdorf (1986), Observations on the effect of temperature rise at fracture in two titanium alloys, *Mater. Sci. Eng.* 77, 85.
- Carslaw, H.S. and J.C. Jaeger (1959), *Conduction of Heat in Solids*, Oxford Press, London.
- Douglas, A.S. and H.U. Mair (1987), The temperature-field surrounding a dynamically propagating mode-III crack, *Scr. Metall.* 21, 479.
- Duffy, J. (1984), Temperature measurements during the formation of shear bands in a structural steel, in: G.J. Dvorak and R.T. Shield, eds., *Mechanics of Material Behavior*, Elsevier, Amsterdam, p. 75.
- Fox, P.G. and J. Sonria-Ruiz (1970), Fracture-induced thermal decomposition in brittle crystalline solids, *Proc. R. Soc. London A317*, 79.
- Freund, L.B. (1977), A simple model of the double cantilever beam crack propagation specimen, *J. Mech. Phys. Solids* 25, 69.
- Giovanola, J.H. (1988a), Adiabatic shear banding under pure shear loading, Part I., *Chem. Mater.* 7, 59.
- Giovanola, J.H. (1988b), Adiabatic shear banding under pure shear loading, Part II, *Mech. Mater.* 7, 73.
- Giovanola, J.H., R.W. Klopp and J.W. Simons (1989), Effect of shear lips on dynamic crack propagation, *Proc. OJI Int. Seminar on Dynamic Fracture*, Toyohashi, Japan, August, 1989.
- Hartley, K.A., J. Duffy and R.H. Hawley (1987), Measurement of the temperature profile during shear band formation in steels deforming at high strain rates, *J. Mech. Phys. Solids* 35, 283.
- Krishna Kumar, R., R. Narasimhan and O. Prabhakar (1991), Temperature rise in a viscoplastic material during dynamic crack growth, *Int. J. Fract.* 48, 23.
- Kuang, Z.-B. and S. Atluri (1985), Temperature field due to a moving heat source: a moving mesh finite element analysis, *J. Appl. Mech.* 52, 277.
- Malali, P.N. (1988), Thermal fields generated by dynamic mode III fracture in ductile materials, M.S. Thesis, The Johns Hopkins University, Baltimore.
- Marchand A. and J. Duffy (1988), An experimental study of the formation process of adiabatic shear bands in a structural steel, *J. Mech. Phys. Solids* 36, 251.
- Mason, J.J. (1993), The mechanism and effects of heat generation at the tip of a dynamic crack or notch. Ph.D. Thesis, California Inst. of Tech., Pasadena, CA, Ch. 2.
- Mason, J.J. and A.J. Rosakis (1992), The effect of hyperbolic heat conduction around a dynamically propagating crack tip, SM Report 92-3, Graduate Aeronautical Laboratories, California Inst. of Tech.
- Mason, J.J., A.J. Rosakis and G. Ravichandran (1992), The conversion of plastic work to heat around a dynamically propagating crack in metals, SM Report 92-17, Graduate Aeronautical Laboratories, California Inst. Tech., Pasadena, CA.
- American Society for Metals (1980), *Metals Handbook*, 9th Ed., Metals Park, OH, Vol. 3, 397.
- Offner, A. (1975), New concepts in projection mask aligners, *Optical Eng.* 14, 130.
- Rice, J.R. and N. Levy (1969), Local heating by plastic deformation at a crack tip, in: A.S. Argon, ed., *Physics of Strength and Plasticity*, MIT Press, Cambridge, MA, p. 277.
- Rosakis, A.J. and A.T. Zehnder (1985), Dynamic fracture initiation and propagation in 4340 steel under impact loading, *Int. J. Fract.* 27, 169.

- Sung, J.C. and J.D. Achenbach (1987), Temperature at a propagating crack tip in a viscoplastic material, *J. Therm. Stresses* 10, 243.
- Taylor, G.I. and M.A. Quinney (1934), The latent energy remaining in a metal after cold working, *Proc. Roy. Soc London A143*, 307.
- Zehnder, A.T. and A.J. Rosakis (1991) On the temperature distribution at the vicinity of dynamically propagating cracks in 4340 steel, *J. Mech. Phys. Solids* 39, 385.
- Zehnder, A.T. and A.J. Rosakis (1992), Temperature rise at the tip of dynamically propagating cracks: measurements using high speed infrared detectors, in: J.S. Epstein, ed., *Experimental Mechanics in Fracture*, III, Society for Experimental Mechanics, Inc., Bethel, CT.
- Zehnder, A.T. and J.A. Kallivayalil (1991), Temperature rise due to dynamic crack growth in beta-c titanium, *Speckle Techniques, Birefringence Methods, and Applications to Solid Mechanics*, (SPIE Vol. 1554A), p. 48.